1984–1989 Nucleic Acids Research, 1995, Vol. 23, No. 11

Energetics of base pair opening in a DNA dodecamer containing an A_3T_3 tract

James G. Moe+, Ewa Folta-Stogniew and Irina M. Russu*

Department of Molecular Biology and Biochemistry, Wesleyan University, Middletown, CT 06459, USA

Received January 30, 1995; Revised and Accepted April 21, 1995

ABSTRACT

Nuclear magnetic resonance spectroscopy has been used to characterize the kinetics and energetics of opening of base pairs in the DNA dodecamer [d(CGCAAATTTGCG)]$_2$. The dodecamer contains an A_3T_3 tract that induces intrinsic curvature of the helix axis. Previous studies from this and other laboratories have shown that the kinetics of base pair opening in A_nT_n tracts is unique: the opening rates of the A·T base pairs in the interior of the tract are much lower than that of the A·T base pair at the 5′-end of the tract. In the present work, we have investigated the energetics of the pathways for opening of the A·T base pairs in the A_3T_3 tract. The energetic parameters of the activated state(s) are obtained from the temperature dependence of the opening rate constants. The lower opening rates for the A·T base pairs situated in the interior of the tract are shown to originate from higher activation enthalpies which are compensated, in part, by increases in the activation entropies. We have also obtained an energetic characterization of the open state(s) of the A·T base pairs in the dodecamer by measuring the equilibrium constants for base pair opening and their temperature dependence. The results suggest that the transitions from closed to open state(s) in the A·T base pairs of the A_3T_3 tract are energetically similar.

INTRODUCTION

The presence of tracts of A·T base pairs has a profound effect on structural and functional properties of DNA. One extreme example is the homopolymer poly(dA)·poly(dT) which has a helical repeat of 10 base pairs per turn (1) and does not undergo the transition from B- to A-DNA upon changes in environmental conditions (2). When embedded in DNA of mixed sequences, short tracts of A·T base pairs, such as A_nT_n and A_n, cause an overall bend in the helix axis as seen, for example, by slow electrophoretic mobility (3,4). The same base sequences show specific patterns of cleavage by the hydroxyl radical (5,6) indicating that they adopt a different conformation.

Crystallographic structures are now available for several DNA dodecamers containing tracts of A·T base pairs of varying lengths (7–11). The structures reveal that the tracts adopt a B′-DNA conformation which is distinct from B-DNA. The B′-DNA conformation is characterized by high propeller twist which maximizes base stacking, narrows the minor groove and could allow for formation of bifurcated hydrogen bonds between adjacent A·T base pairs across the major groove. A network of ordered water molecules was observed in the minor groove (7,11) and its geometry was predicted to depend on the width of the groove (12). The high propeller twist, and the resulting enhancement in stacking interactions, are believed to be major determinants of the intrinsic curvature of these DNA base sequences (13).

Nuclear magnetic resonance (NMR) spectroscopy studies have revealed an unique dynamic behavior of tracts of A·T base pairs (14,15). For all DNA fragments studied, the A·T base pair at the 5′-end of the tract has a high opening rate (i.e. >100 s^{-1} at room temperature). For A·T base pairs situated in the interior of the tract, the opening rates are greatly lowered. This kinetic behavior is present when the tract contains more than four consecutive A·T base pairs (which may include a 5′-AT-3′ step but not a 5′-TA-3′ step) and is directly correlated to DNA curvature (14). An energetic coupling between DNA bending and base pair opening has also been inferred from molecular modeling studies (16).

In order to understand the origin of the unique base pair opening kinetics in A_nT_n tracts, in the present work, we have investigated the energetics of opening of A·T base pairs in the dodecamer [d(CGCAAATTTGCG)]$_2$. This oligonucleotide has been extensively characterized and has become a model for DNA containing A_nT_n tracts. Structures of the dodecamer have been obtained by X-ray diffraction techniques at 2.5 and 2.2 Å resolution (8,11). Interaction of the dodecamer with distamycin A has been characterized in solution state by NMR methods (17,18). In our laboratory we have obtained the kinetics of base pair opening in this dodecamer at room temperature (15). In the present work, we are extending our previous investigation by a study of the temperature dependence of the rate constants and equilibrium constants for base pair opening in the dodecamer.

MATERIALS AND METHODS

Sample preparation

The dodecamer was synthesized using the solid-support phosphoramidite method and was purified by reverse-phase high pressure liquid chromatography on a PRP-1 column (Hamilton)

* To whom correspondence should be addressed

+Present address: GENE-TRAK, 31 New York Avenue, Framingham, MA 01701, USA

in 50 mM ethylene diamine formate buffer at pH 7.5 with a gradient of 0–25% acetonitrile over 25 min.

The purified oligonucleotide was dialyzed extensively against 0.6 M NaCl to exchange the counterion to sodium and then, was dialyzed with four exchanges against 2 mM ammonia buffer containing 0.1 M NaCl, 2 mM EDTA, 10% D_2O, pH 8.73 at 25°C. The dialysis buffer contained Chelex 100 (100–200 mesh, sodium form, Bio-Rad) to remove traces of metal ions from the sample. Various concentrations of ammonia were obtained by titrating the sample with Chelex-treated stock solutions of either 0.4 or 2 M ammonia buffer containing 0.1 M NaCl, 2 mM EDTA, pH 8.73 at 25°C. The final DNA concentration was ~0.75 mM (duplex).

NMR experiments

^{1}H NMR experiments were carried out on a Varian VXR-400/54 NMR spectrometer operating at 400 MHz. All spectra were referenced to 2,2-dimethyl-2-silapentane-5-sulfonate (DSS) as an external reference. The imino proton resonances were observed using the 1–3–3–1 pulse (19) or the Jump-and-Return pulse (20). Longitudinal relaxation times (T_1) were measured by the selective saturation-recovery method with 12–15 values for the recovery delay following saturation of individual resonances. The T_1 values were obtained from exponential non-linear least-squares fits of intensity as a function of recovery delay.

Calculation of the parameters of interest

The T_1 value of an imino proton is related to its rate of exchange, k_{ex}, by: $1/T_1 = k_{ex} + 1/T_1^0$, where T_1^0 is the longitudinal relaxation time corresponding to mechanisms other than exchange (e.g., proton–proton dipolar interactions). The exchange occurs from an open state of the base pair in which the imino groups are accessible to solvent and the inter-base hydrogen bonds are broken. Exchange from the open state is base-catalyzed. Thus, the overall exchange rate depends on the concentration of base catalyst [B], the rate constants for opening and closing of the base pair, k_{op} and k_{cl}, respectively, and the rate constant k_B for transfer of the imino proton from the open base pair to the catalyst. This dependence is expressed as (21):

$$k_{ex} = \frac{k_{op} \cdot k_B \cdot [B]}{k_{cl} + k_B \cdot [B]} \quad (1)$$

Accordingly, the T_1 value of the imino proton is (15):

$$T_1 = \frac{T_1^0(\tau_0 + D \cdot [B]^{-1})}{T_1^0 + \tau_0 + D \cdot [B]^{-1}} \quad (2)$$

where, $\tau_0 = 1/k_{op}$ is the lifetime of the base pair in the closed state, and D is a constant defined as $(K_{op} \cdot k_B)^{-1}$ in which K_{op} is the equilibrium constant for formation of the open state ($K_{op} = k_{op}/k_{cl}$).

The experimental T_1 values were fitted as a function of the inverse of the concentration of base catalyst (ammonia) to Equation (2) using a non-linear least-squares program. The fitted parameters were the base pair lifetime, τ_0, constant D and relaxation time, T_1^0. The concentration of base catalyst was calculated as the fraction $\{1/(1 + 10^{(pK-pH)})\}$ of the total ammonia concentration. The change in the pK value of ammonia with temperature was calculated using a standard enthalpy of ionization of 12.4 Kcal/mol (*CRC Handbook of Chemistry and Physics*, 1986). The pH of the buffer was measured at each temperature of interest.

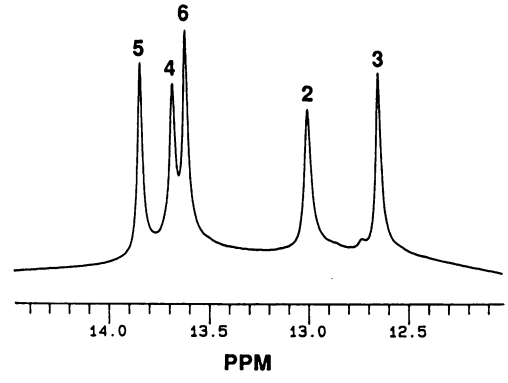

Figure 1. Imino proton resonances of the dodecamer in 10 mM ammonia buffer containing 100 mM NaCl and 2 mM EDTA at pH 8.9 and at 20°C. Assignments of resonances to individual protons are indicated according to the following numbering of base pairs:

```
      23456
5'-d(CGCAAATTTGCG)-3'
3'- (GCGTTTAAACGA)d-5'
        65432
```

At 20°C, the imino proton resonance of the terminal C·G base pairs is not observed due to fraying at the ends of the duplex.

The activation enthalpy, $\Delta H^{\ddagger 0}$, and the activation entropy, $\Delta S^{\ddagger 0}$, for base pair opening were calculated from the temperature dependence of the opening rate constants based on Eyring equation (22):

$$\ln(k_{op}/T) = \ln(\kappa \cdot k/h) + \Delta S^{\ddagger 0}/R - \Delta H^{\ddagger 0}/RT \quad (3)$$

where T is the absolute temperature, k is Boltzmann's constant, h is Planck's constant and R is the gas constant. The transmission coefficient, κ, was assumed to have a value of 1.

The equilibrium constants for base pair opening were obtained from the constant D as $K_{op} = 1/(D \cdot k_B)$. A catalytic rate constant k_B of $1.3 \cdot 10^8$/M/s was used for each base pair. This value is 1.5 lower than the rate constant in free nucleosides (23) in order to correct for the lower diffusion coefficient of the imino proton in DNA (24,25).

The standard enthalpy change, ΔH^0, and the standard entropy change, ΔS^0, for formation of the open state of the base pair were calculated from van't Hoff equation:

$$\ln(K_{op}) = -\Delta H^0/RT + \Delta S^0/R \quad (4)$$

All errors reported in the paper represent one standard deviation in the least-squares analysis.

RESULTS AND DISCUSSION

Rate constants and activation parameters for base pair opening

The imino proton resonances of the dodecamer are shown in Figure 1. The assignments of the resonances to individual base pairs were obtained previously by this laboratory (15,26).

The selective T_1 of each imino proton was measured as a function of the concentration of ammonia at five temperatures

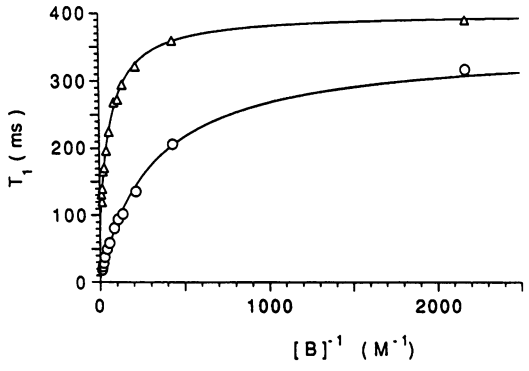

Figure 2. Dependence of the T_1 values of imino protons in A·T4 (circles) and A·T6 (triangles) base pairs on the inverse of ammonia base concentration at 20°C. The curves correspond to non-linear least-squares fits to Equation 2.

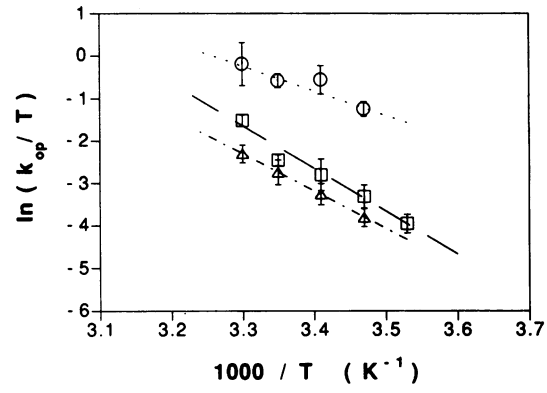

Figure 3. Dependence of the rate constants for opening of A·T base pairs in the dodecamer on temperature: A·T4 (circles), A·T5 (squares) and A·T6 (triangles).

between 10 and 30°C. Over this temperature range, the dodecamer is well below its melting temperature (namely, 66°C in 10 mM phosphate buffer + 0.1 M NaCl and 2 mM EDTA, pH 7.0, as measured from the melting transitions observed in the NMR spectra). Hence, strand dissociation does not contribute significantly to the measured exchange rates. An illustration of the dependence of the T_1 values on the concentration of ammonia base is shown in Figure 2. Representative values of the rate constants for base pair opening are given in Table 1. The opening rate constants for base pairs C·G1 and G·C2 are not reported since, over the temperature range of interest, they are affected by fraying at the ends of the duplex. As seen in Table 1, the opening rate for the A·T base pair at the 5′-end of the A_3T_3 tract is increased 6–9-fold relative to those of central A·T base pairs. This trend is maintained over the entire temperature range investigated (Fig. 3). (At 10°C, the imino proton resonances of A·T4 and A·T6 overlap. We have attempted to calculate the T_1 value for each of these imino protons by fitting the intensity of the overlapped resonance as a function of the recovery delay to a sum of two exponential functions. Over a wide range of base catalyst concentrations, this procedure could not resolve the individual T_1 values, most likely due to the fact that the T_1 values were not sufficiently different. Consequently, determinations of the opening rates and equilibrium constants for these base pairs at 10°C were not sufficiently accurate and the values are not reported.) The activation parameters for opening, derived from the temperature-dependence of the opening rates (Equation 3), are summarized in Table 2. [The larger errors for $\Delta S^{\ddagger 0}$ result from the equation used for their calculation (Equation 3). Both the y-intercept of $\ln(k_{op}/T)$ versus 1/T and $\ln(k/h)$ are large numbers and their difference, from which $\Delta S^{\ddagger 0}$ is calculated, is small. As a result, the errors in the y-intercept propagate into larger relative errors for $\Delta S^{\ddagger 0}$ values.] The activation enthalpy for the A·T5 base pair is, within experimental error, the same as that of A·T6. The value is comparable with activation energies previously found for the central A·T base pairs in $[d(GGAAATTTCC)]_2$ and for a homopolymer containing 14 A·T base pairs (14). In contrast, for the A·T base pair at the 5′-end of the A_3T_3 tract (A·T4), the activation enthalpy is decreased by 6–9 kcal/mol relative to those of the central base pairs. Its value is comparable with activation enthalpies for opening of A·T base pairs in 'random' base sequences. For example, we have recently found that, in the dodecamer $[d(CGCAGATCTGCG)]_2$, the two A·T base pairs have activation enthalpies for opening of 8 ± 2 and 7 ± 2 kcal/mol, respectively (27). Similarly, the A·T base pairs in the decamer $[d(CGCGATCGCG)]_2$ have an activation enthalpy of 10 kcal/mol (21). These results suggest that, the activated state during opening of the A·T base pair at the 5′-end of the A_3T_3 tract resembles that of an A·T base pair in a 'random' base sequence and is different from those of the base pairs within the tract. The existence of these energetic variations among A·T base pairs within A_nT_n tracts appears to depend on the length of the tract. For example, previous results from our laboratory have shown that in two dodecamers containing A_2T_2 tracts, namely, $[d(CGCGAATTCGCG)]_2$ and $[d(CGCGAATTTGCG)]_2$, the activation energies of both A·T base pairs are high (i.e., 18–20 kcal/mol) (25). Thus, the enthalpic destabilization of the activated state for the base pair at the 5′-end of the A_nT_n tract may require at least three A·T base pairs followed by three T·A base pairs ($n \geq 3$).

Table 1. Base pair opening rates, k_{op}, in ammonia buffer containing 100 mM NaCl and 2 mM EDTA at pH 8.73 and at 25°C

Base pair	G·C3	A·T4	A·T5	A·T6
$k_{op}(s^{-1})$	59 ± 35	167 ± 28	26 ± 3	19 ± 5

Table 2. Activation parameters for base pair opening in the $[d(CGCAAATTTGCG)]_2$ dodecamer

Base pair	$\Delta H^{\ddagger 0}$ (kcal/mol)	$\Delta S^{\ddagger 0}$ (cal/mol·K)
G·C3	22 ± 5	25 ± 16
A·T4	11 ± 4	−10 ± 12
A·T5	20 ± 2	16 ± 6
A·T6	17 ± 3	6 ± 11

The energetic parameters measured in the present work do not provide details about the conformational features associated with the activated state(s) during opening of A·T base pairs in the A_3T_3 tract. Generally, base pair opening in double-stranded DNA is believed to involve unstacking of the bases, breakage of inter-base hydrogen bonds and deformation of the sugar–phosphate

backbone (16,28,29). All these processes are expected to contribute, to various extents, to the observed activation enthalpies (30). For the dodecamer of interest here, the crystallographic structures show that the central A·T base pairs have large concerted propeller twists which result in enhanced stacking for these base pairs. Moreover, in at least one of the central adenines, the N-6 amino group could form bifurcated hydrogen bonds to O-4 atoms on two succesive thymines (8,11). The enhanced stacking and, possibly, the presence of bifurcated hydrogen bonds in the closed state should result in higher activation enthalpies for opening of the central A·T base pairs.

The activation entropies for base pair opening show a parallel trend to that observed for the activation enthalpies. The $\Delta S^{\ddagger 0}$ values for the central A·T5 and A·T6 base pairs are larger than that for the A·T base pair at the 5′-end of the tract. For the latter A·T base pair, the activation entropy is negative (or close to zero). The relationship between $\Delta H^{\ddagger 0}$ and $\Delta S^{\ddagger 0}$ values is illustrated in Figure 4. Clearly, for all base pairs investigated, the activation enthalpies are linearly related to the activation entropies. Thus, decreases in activation enthalpy which should favor opening are, in part, compensated by parallel decreases in activation entropy. Due to this enthalpy/entropy compensation, the variations in the opening rates among base pairs are attenuated. For example, the lower activation enthalpy for the A·T4 base pair should be expected to increase the opening rate of this base pair by a factor of 10^4–10^6 relative to those of the other A·T base pairs in the dodecamer. As shown in Table 1, the opening rates for A·T4 base pair are, in fact, only 6–9-fold greater than those of A·T5 and A·T6. Thus, the enthalpy/entropy compensation in the formation of the activated state results in an energetic balance that limits the range of values allowed for base pair opening rates. Enthalpy/entropy compensation in base pair opening in DNA has been recently demonstrated by this laboratory for the dodecamers $[d(CGCACATGTGCG)]_2$ and $[d(CGCAGATCTGCG)]_2$ (27). The results for these two dodecamers are included in Figure 4. They are in excellent agreement to those obtained in the present work suggesting that enthalpy/entropy compensation is a general feature of base pair opening in DNA.

Enthalpy/entropy compensation has been observed in a variety of processes involving nucleic acids and their interactions with ligands (31,32). Yet, the molecular basis of this thermodynamic behavior is not fully understood. Enthalpy/entropy compensation is evident in coil–helix transitions of single strands, hairpins and duplexes of DNA and RNA (31). For these transitions, the enthalpy changes have been attributed mainly to stacking interactions whereas the entropy changes have been attributed to restrictions of internal rotations within the sugar–phosphate backbone of the helix (31). To observe enthalpy/entropy compensation, stronger stacking interactions should be associated with smaller residual torsional motions of the phosphodiester bonds. This model is, in part, consistent with our present findings. As explained above, the larger activation enthalpies for opening of the central A·T base pairs (Table 2) could result from the enhanced stacking of these base pairs observed in the crystallographic structures of the dodecamer (8,11). However, the increased rigidity of the sugar–phosphate backbone within the A_3T_3 tract, predicted by the model, has not yet been fully demonstrated. Enthalpy/entropy compensation in base pair opening in DNA may also reflect contributions from DNA

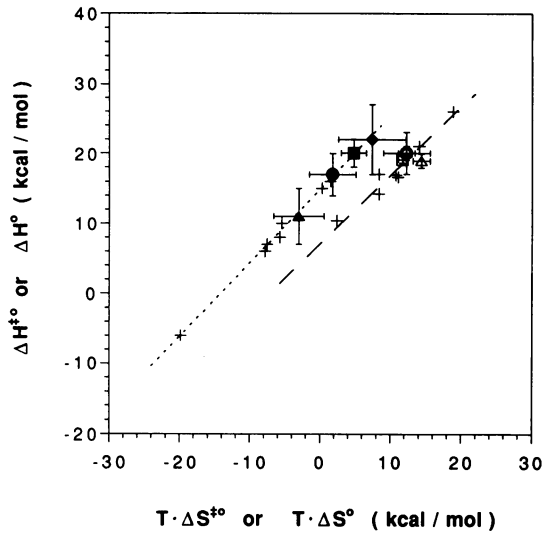

Figure 4. Enthalpy–entropy compensation in base pair opening in the dodecamer investigated (T = 300 K). Filled symbols: activation parameters; open symbols: equilibrium parameters. C·G3 (diamonds); A·T4 (circles); A·T5 (squares) and A·T6 (triangles). The crosses represent the corresponding enthalpy and entropy changes for opening of base pairs in positions 3–6 in the dodecamers $[d(CGCACATGTGCG)]_2$ and $[d(CGCAGATCTGCG)]_2$ [from (27)].

hydration. Positive entropy contributions from the solvent have been proposed as thermodynamic forces in interactions of ligands with proteins and DNA (32–35). If one assumes that formation of the activated state during opening of the base pair disrupts the hydration shell(s) and releases water molecules, activation enthalpies should be correlated to activation entropies. If this is the case, the higher activation enthalpies observed here for the central A·T base pairs in the dodecamer may be explained by a higher level of hydration for these base pairs, similar to that observed experimentally for poly(dA)·poly(dT) (36).

Equilibria between open and closed states of the base pairs

The equilibrium constants for opening, K_{op} show a dependence on the location of the base pair in the A_3T_3 tract similar to that observed for opening rates (Fig. 5). The equilibrium constants for the central A·T5 and A·T6 base pairs are comparable and they are both decreased 4–7-fold relative to that of the A·T4 base pair. This result suggests that the rate constants for closing are similar and the differences in the equilibrium constants originate mainly from differences in the opening rates.

The standard enthalpy and entropy changes for opening, obtained from the van't Hoff analysis of the K_{op} values (Equation 4), are the same for all base pairs in the dodecamer (Table 3). Thus, the overall pathways from closed to open state for the A·T base pairs in this dodecamer appear to be similar. When the standard enthalpy and entropy changes in the dodecamer investigated are compared to those in the dodecamers $[d(CGCACATGTGCG)]_2$ and $[d(CGCAGATCTGCG)]_2$ (27), the values fall within the correlation previously seen (Fig. 4). This finding suggests that enthalpy/entropy compensation is present also in the equilibrium between closed and open states.

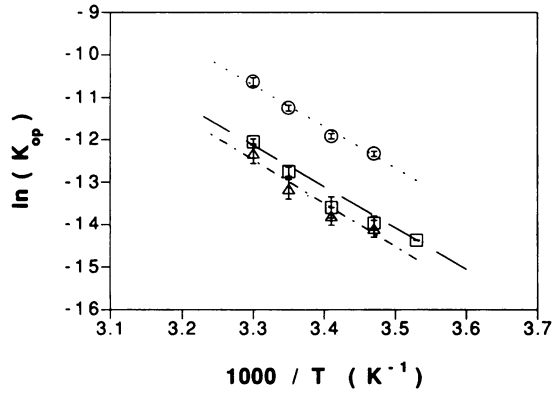

Figure 5. Dependence of the equilibrium constants for opening of A·T base pairs on temperature: A·T4 (circles), A·T5 (squares) and A·T6 (triangles).

Table 3. Thermodynamic parameters for base pair opening in the $[d(CGCAAATTTGCG)]_2$ dodecamer

Base pair	ΔH^0 (kcal/mol)	ΔS^0 (cal/mol·K)
G·C3	20 ± 1	41 ± 4
A·T4	19 ± 1	43 ± 4
A·T5	19.2 ± 0.5	39 ± 2
A·T6	20 ± 3	42 ± 11

Previous work from other laboratories has used the energetics of helix–coil transition to evaluate the contributions of individual base pairs to the stability of DNA structures (37). The results indicated that the stability of the DNA duplex can be predicted from the base sequence as the sum of nearest-neighbor pairwise interactions. In the processes of base pair opening investigated in the present work, two such nearest-neighbor interactions are expected to be perturbed. Thus, the enthalpy changes derived from helix–coil transitions (37) can be used to predict the standard enthalpy changes for formation of the open state of each base pair in the dodecamer of interest. The predicted values (16.9 kcal/mol for G·C3, 14.9 kcal/mol for A·T4, 18.2 kcal/mol for A·T5 and 17.7 kcal/mol for A·T6) are lower than the measured standard enthalpy changes for opening (Table 3). The largest difference is observed for A·T4, i.e., 14.9 kcal/mol predicted versus (19 ± 1) kcal/mol measured. These differences support the suggestion that the open state of the base pair probed by imino proton exchange differs from the unstacked open state observed in the helix–coil transition (24). Moreover, sequence-induced structural variations in the dodecamer of interest may also contribute to the observed differences.

New insight into the processes of base pair opening at temperatures below the helix–coil transition is obtained by comparing the energetic parameters of the activated state with those of the open state (Table 2 and 3). The standard enthalpy changes for opening of the central A·T5 and A·T6 base pairs are, within experimental errors, the same as the activation enthalpies. Thus, for these base pairs, no enthalpic destabilization occurs in going from the activated to the open state. In contrast, for the A·T4 base pair, the standard enthalpy change exceeds the activation enthalpy by ~8 kcal/mol. A possible explanation for this difference is suggested by the theoretical molecular modeling of opening of the central A·T base pair in $(dA)_5.(dT)_5$ (16). When no bending of the DNA was allowed, the energy of opening the central thymine towards the major groove was found to increase monotonically with the opening angle reaching a value of ~20 kcal/mol at an opening angle of ~25°. On the other hand, for bent DNA (of a radius of curvature of 20 Å), once an opening angle of 15° was reached, the energy became much less dependent on further increases in the opening angle. In the frame of these theoretical results, the pathway for opening of the A·T4 base pair in the dodecamer resembles that in straight DNA. For the central A·T base pairs, one could postulate that the activation state corresponds to an opening angle of 15° in bent DNA and thus, no further changes in the enthalpy should occur in going from the activated to the open state.

Our present results also show that transition from the activated to the open state involves increases in entropy for all base pairs. Several processes may be expected to contribute to this effect. First, the base(s) may gain translational and rotational freedom on the pathway from the activated to the open state. Secondly, formation of the open state could be expected to result in further disturbances of water molecules in the DNA hydration shell(s) and thus, contibute to a positive entropy change. A complete answer to this question awaits molecular mechanics and molecular dynamics simulations of base pair opening in the dodecamer and related DNA oligonucleotides.

CONCLUSIONS

The results obtained in the present work indicate that the energetics of the molecular pathway for opening of A·T base pairs in an A_3T_3 tract is strongly dependent on the location of the pair in the tract. The A·T base pair at the 5′-end of A_3T_3 tract has the lowest activation enthalpy and activation entropy. For the A·T base pairs within the A_3T_3 tract, formation of the activated state involves larger enthalpy and entropy changes. The net balance between these two opposite energetic effects yields lower opening rates for the central A·T base pairs.

Transition from the activated to the open state involves, for all base pairs, increases in the entropy. These entropy changes compensate for any enthalpic destabilization of the open state relative to the activated state such as that observed for the A·T base pair at the 5′-end of A_3T_3 tract. Overall, the processes involved in formation of the open states of the A·T and G·C base pairs in the dodecamer are energetically similar.

REFERENCES

1 Rhodes, D., and Klug, A. (1981) *Nature (London)*, **292**, 378–380.
2 Leslie, A. G. W., Arnott, S., Chandrasekaran, R., and Ratliff, R. L. (1980) *J. Mol. Biol.*, **143**, 49–72.
3 Crothers, D. M., Haran, T. E., and Nadeau, J. G. (1990) *J. Biol. Chem.*, **265**, 7093–7096.
4 Hagerman, P. J. (1990) *Annu. Rev. Biochem.*, **59**, 755–781.
5 Burkhoff, A. M., and Tullius, T. D. (1987) *Cell* **48**, 935–943.
6 Burkhoff, A. M., and Tullius, T. D. (1988) *Nature (London)*, **331**, 455–457.
7 Dickerson, R. D., and Drew, H. R. (1981) *J. Mol. Biol.*, **149**, 761–786.
8 Coll, M., Frederick, C. A., Wang, A. H.-J., and Rich, A. (1987) *Proc. Natl. Acad. Sci. USA*, **84**, 8385–8389.
9 Nelson, H. C. M., Finch, J. T., Luisi, B. F., and Klug, A. (1987) *Nature (London)*, **330**, 221–226.

10 DiGabriele, A. D., Sanderson, M. R., and Steitz, T. A. (1989) *Proc. Natl. Acad. Sci. USA*, **86**, 1816–1820.
11 Edwards, K. J., Brown, D. G., Spink, N., Skelly, J. V., and Neidle, S. (1992) *J. Mol. Biol.*, **226**, 1161–1173.
12 Chuprina, V. P., Heinemann, U., Nurislamov, A. A., Zielenkiewicz, P., Dickerson, R. E., and Saenger, W. (1991) *Proc. Natl. Acad. Sci. USA*, **88**, 593–597.
13 Diekmann, S., Mazzarelli, J. M., McLaughlin, L. W., von Kitzing, E., and Travers, A. A. (1992) *J. Mol. Biol.* **225**, 729–738.
14 Leroy, J.-L., Charretier, E., Kochoyan, M., and Gueron, M.(1988) *Biochemistry*, **27**, 8894–8898.
15 Moe, J. G., and Russu, I. M. (1990) *Nucleic Acids Res.* **18**, 821–827.
16 Ramstein, J., and Lavery, R. (1988) *Proc. Natl. Acad. Sci. USA*, **85**, 7231–7235.
17 Pelton, J. G., and Wemmer, D. E. (1989) *Proc. Natl. Acad. Sci. USA*, **86**, 5723–5727.
18 Pelton, J. G., and Wemmer, D. E. (1990) *J. Am. Chem. Soc.*, **112**, 1393–1399.
19 Hore, P. J. (1983) *J. Magn. Res.*, **55**, 283–300.
20 Plateau, P., and Gueron, M. (1982) *J. Am. Chem. Soc.*, **104**, 7310–7311.
21 Leroy, J. L., Kochoyan, M., Huynh-Dinh, T., and Gueron, M. (1988) *J. Mol. Biol.*, **200**, 223–238.
22 Glasstone, S., Laidler, K. J., and Eyring H. (1941) *The Theory of Rate Processes. The Kinetics of Chemical Reactions, Viscosity, Diffusion and Electrochemical Phenomena*. McGraw-Hill, New York and London.
23 Gueron, M., Charretier, E., Hagerhorst, J., Kochoyan, M., Leroy, J.-L., and Moraillon, A. (1990) In *Structure and Methods*. Sarma, R. H., and Sarma, M. H., (eds), Adenine Press, Vol. 3, pp. 113–137.
24 Benight, A. S., Schurr, J. M., Flynn, P. F., Reid, B. R., and Wemmer, D. E. (1988) *J. Mol. Biol.*, **200**, 377–399.
25 Moe, J. G., and Russu, I. M. (1992) *Biochemistry*, **31**, 8421–8428.
26 Michalczyk, R., and Russu, I. M. (1993) *FEBS Lett.*, **331**, 217–222.
27 Folta-Stogniew, E., and Russu, I. M. (1994) *Biochemistry*, **33**, 11016–11024.
28 Keepers, J. W., Kollman, P. A., Weiner, P. K., and James, T. L. (1982) *Proc. Natl. Acad. Sci. USA*, **79**, 5537–5541.
29 Briki, F., Ramstein, J., Lavery, R., and Genest, D. (1991) *J. Am. Chem. Soc.*, **113**, 2490–2493.
30 Englander, S. W., and Kallenbach, N. R. (1984) *Quart. Rev. Biophys.*, **16**, 521–655.
31 Searle, M. S., and Williams, D. H. (1993) *Nucleic Acids Res.*, **21**, 2051–2056.
32 Breslauer, K. J., Remeta, D. P., Chou, W.-Y., Ferrante, R., Curry, J., Zaunczkowski, D., Snyder, J. G., and Marky, L. A. (1987) *Proc. Natl. Acad. Sci. USA*, **84**, 8922–8926.
33 Lumry, R., and Rajender, S. (1970) *Biopolymers*, **9**, 1125–1227.
34 Marky, L. A., and Breslauer, K. J. (1987) *Proc. Natl. Acad. Sci. USA*, **84**, 4359–4363.
35 Berman, H. M. (1986) *Transactions ACA*, **22**, 107–119.
36 Pilet, J., Blicharski, J., and Brahms, J. (1975) *Biochemistry*, **14**, 1869–1876.
37 Breslauer, K. J., Frank, R., Blocker, H., and Marky, L. A. (1986) *Proc. Natl. Acad. Sci. USA*, **83**, 3746–3750.